# A Mechanism for Ion Transport across the Water/Dichloromethane Interface: A Molecular Dynamics Study Using Polarizable Potential Models

**Liem X. Dang**

*P.O. Box 999 Mail Stop K8-91, Environmental Molecular Sciences Laboratory, Pacific Northwest National Laboratory, Richland, Washington 99352*

*Received: October 27, 2000*

In this work, we used molecular dynamics techniques and potential of mean force approaches to compute the ion transfer free energy for the water/dichloromethane liquid−liquid interface. We used polarizable potential models to describe the interactions among the species. Both forward and reverse directions simulations were carried out to evaluate the differences in the free energy profiles. On the basis of the results of our calculations, we have proposed a mechanism that describes the transport of a chloride ion across the interface. The computed ion transfer free energy is $14 \pm 2$ kcal/mol, which is in qualitative agreement with the experimentally reported value of $10 \pm 1$ kcal/mol. A smooth transition from the aqueous phase to the nonaqueous phase on the free energy profile clearly indicates that the ion transfer mechanism is a nonactivated process. The computed hydration number for the chloride ion indicates that some water molecules are associated with the ion inside the nonaqueous phase. This result is in excellent agreement with the experimental interpretation of the ion transfer mechanism reported recently by Osakai et al. (*J. Phys. Chem.* **1997**, *101*, 8341).

## I. Introduction

Computer simulation has been used extensively to compute free energy profiles or the potentials of mean force (PMF) for complex processes in solution. These studies have made valuable contributions to the overall understanding of the physics and chemistry of solvation. Examples of studies that have been undertaken include free energy calculations for ion pairs in water,[1] crown ether−cation associations in aqueous solution,[2] methane pair in water,[3] as well as the PMF benzene−benzene association in aqueous solution.[4] In addition to enabling comparisons between the computational results with data obtained from experiments, these studies have provided insight into molecular-level association processes in solutions. This approach has recently been extended to studies of ion transport across liquid−liquid interfaces. The process of ion transport across the interface between water and an immiscible organic solvent is of great interest, not only because of its fundamental importance in chemical and biological systems but also because it is a diverse and rich phenomenon. The study of ion transfer is also very important to environmental problems such as the interactions of contaminated organic solvents with groundwater and separation chemistry performed in binary solvent systems.[5]

Interest in computer simulation of ion transport has intensified since Benjamin published the results of his work on the mechanism and dynamics of transferring a single chloride ion across a water/1,2-dichloroethane interface.[6] Because of approximations made on the electrostatic free energy calculation, Benjamin suggested that, due to the presence of a free energy minimum (∼5 kcal/mol) at the liquid−liquid interface, ion transfer into the aqueous phase is an activated process. Schweighfer and Benjamin recently studied transport of the ammonium ion from water to the nitrobenzene liquid−liquid interface and found no barrier when the system is fully equilibrated.[7] In a paper describing their molecular dynamics study on the structural and energetic characteristics of ion-assisted transfer between water and chloroform, Lauterbach et al. report that the cesium ion diffuses spontaneously from the interface to water and displays apparently no free energy minimum.[8] Recently, Fernandes and co-workers reported a series of molecular dynamics simulations on ion transfer processes from water to organic solvents. Their computed ion transfer free energies are in reasonable agreement with the experimental data, and no minima were observed at the liquid−liquid interface.[9]

We recently published the results of study in which we used molecular dynamics techniques and polarizable potential models to study the mechanism for transporting a chloride ion or a cesium ion across a water/carbon tetrachloride liquid−liquid interface.[10] The results obtained in these studies provided new insight into both the free energies and solvent structures as the ions moved across the interface. The computed free energy profiles of ion transfer for both ions increased monotonically from water to carbon tetrachloride, and no free energy minima were observed at the liquid−liquid interface. The first hydration shells of the ions were significantly reduced as the ions moved from the aqueous phase to the nonaqueous phase. Fingering effects were created by the ion in the nonaqueous phase. These fingering effects have characteristics similar to those found in previous work.[6,7] There is no experimental data available for this system due to its low dielectric permittivity; therefore, we were unable to compare our computed free energy results for the ion transfer processes with experimental data.

In this paper, we discuss our study of the mechanism of transferring a chloride ion across the water/dichloromethane liquid−liquid interface. Dichloromethane, a dipolar, aprotic liquid with a simple molecular structure, has been widely used as a solvent in the processing of radioactive materials and contributes significantly to nuclear waste remediation problems.[5] There are two main reasons why we undertook this work. First, by characterizing molecular processes at interfaces, our understanding of environmental restoration issues will be furthered. In addition, there is experimental data available for the ion transfer free energy in this system. Second, comparison of our results with the corresponding experimental data will enable

10.1021/jp003991b CCC: $20.00 
Published on Web 12/28/2000

**TABLE 1: Potential Parameters for $CH_2Cl_2$, $H_2O$, and $Cl^-$ Used in the MD Simulations[a]**

| molecule | atom type | $\sigma$ (Å) | $\epsilon$ (kcal/mol) | $q$ (e) | $\alpha$ (Å$^3$) |
|---|---|---|---|---|---|
| $CH_2Cl_2$ | C | 3.410 | 0.137 | −0.2720 | 0.878 |
| | H | 2.400 | 0.040 | −0.0537 | 0.135 |
| | Cl | 3.450 | 0.280 | 0.1897 | 1.910 |
| $H_2O$ | H | 0.000 | 0.0000 | 0.5190 | 0.000 |
| | O | 3.234 | 0.1825 | 0.0000 | 0.000 |
| | M | 0.000 | 0.0000 | −1.0380 | 1.440[b] |
| $Cl^-$ | Cl | 4.410 | 0.1000 | −1.0000 | 3.690 |

The potential parameters are taken from refs 11 and 13. $\sigma$ and $\epsilon$ are the Lennard-Jones parameters, q is the atomic charge, and $\alpha$ is the atomic polarizability. Reference 12.

us to quantify our approach and help in further developing accurate potential energy surfaces.

This paper is organized as follows. The polarizable model potentials and the method of simulation are summarized in Section II. Free-energy profiles and the solvation properties of the liquid−liquid interface are presented and discussed in Section III. Our conclusions and discussion of future research directions are presented in Section IV.

## II. Potential Models and Computational Methods

Our molecular dynamics model for polarizable water is a rigid, four-site, polarizable model.[11] The monomer geometry is represented using gas-phase values obtained by experiment. Fixed charges are assigned to hydrogen atoms and to the point (M) on the bisector of the H−O−H angle that is 0.215 Å away from the oxygen atom. The M point also carries a polarizability ($\alpha = 1.44$ Å$^3$)[12] to describe polarization effects. This potential was constructed to reproduce the thermodynamic and dynamical properties of clusters and bulk liquid water as well as selected properties of the water liquid−vapor interface. A rigid five-site, all-atom interaction potential is used for dichloromethane.[13] Fixed atomic charges and Lennard-Jones potential parameters are assigned to each atom to describe the intermolecular van der Waals and Coulombic interactions. In addition, point polarizabilities[14] are associated with each atom to account for the nonadditive induced polarization effect. This potential was constructed to reproduce the thermodynamic and dynamical properties of clusters and bulk liquid dichloromethane as well as some selected properties of the dichloromethane liquid−vapor interface. The cross interaction (i.e., Lennard-Jones term) between $CH_2Cl_2$ and $H_2O$ molecules was obtained via the Lorentz−Berthelot combining rule.[15] In the lowest-energy structure of $CH_2Cl_2-H_2O$ dimer, two hydrogen atoms of the $CH_2Cl_2$ are facing toward the water molecule while the two chloride atoms are pointing away from the water molecule. The binding energy for the $CH_2Cl_2-H_2O$ dimer is −2.3 kcal /mol, which is slightly stronger than the corresponding $CCl_4-H_2O$ interaction.[16] Simulations of the water/dichloromethane liquid−liquid interface were performed using these potential models. Reasonable results were obtained from these simulations for equilibrium properties such as the density profiles and surface tension.[13]

The chloride ion potential parameters ($Cl^-−H_2O$) are taken from our earlier work on ion solvation in aqueous solution. The predicted minimum structure and energies are in good agreement with high-level electronic structure calculations.[17] Other researchers have proposed a different set for ($Cl^-−H_2O$) potential models.[18] The Lorentz−Berthelot combining rule was used to determine the interactions between $Cl^-−CH_2Cl_2$ (i.e., $Cl^-−C$, $Cl^-−H$, and Cl−Cl). A summary of the $Cl^-−H_2O$ and $Cl^-−CH_2Cl_2$ interaction energies as a function of ion−molecule separation is shown in Figure 1.

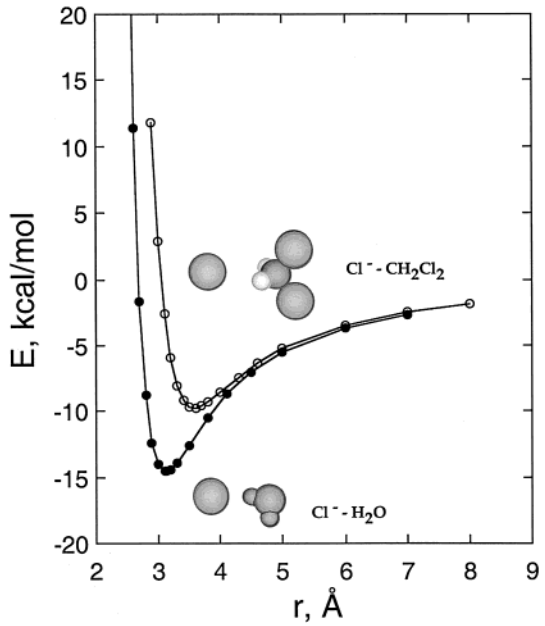


**Figure 1.** Gas-phase $Cl^-−H_2O$ and $Cl^-−CH_2Cl_2$ interaction energies as a function of ion−molecule separations. Insets are the lowest-energy structures.

The total interaction energy of the system is summarized as follows:

$$U_{tot} = U_{pair} + U_{pol} \quad (1)$$

$$U_{pair} = \sum_i \sum_j \left( 4\epsilon \left[ \left( \frac{\sigma_{ij}}{r_{ij}} \right)^{12} - \left( \frac{\sigma_{ij}}{r_{ij}} \right)^{6} \right] + \frac{q_i q_j}{r_{ij}} \right) \quad (2)$$

and

$$U_{pol} = -\sum_{i=1}^{N} \mu_i E_i^0 - \frac{1}{2} \sum_{i=1}^{N} \sum_{j=1, i \neq j}^{N} \mu_i T_{ij} \mu_j + \sum_{i=1}^{N} \frac{|\mu_i|^2}{2\alpha_i} \quad (3)$$

Here, $r_{ij}$ is the distance between site $i$ and $j$, $q$ is the charge, and $\sigma$ and $\epsilon$ are the Lennard-Jones parameters. The term $E_i^0$ is the electric field at site $i$ produced by the fixed charges in the system, $\mu_i$ is the induced dipole moment at atom site $i$, and $T_{ij}$ is the dipole tensor. The first term in eq 3 represents the charge−dipole interaction, the second term describes the dipole−dipole interaction, and the last term is the energy associated with the generation of the dipole moment $\mu_i$. During molecular dynamics simulations, a standard iterative, self-consistent field procedure is used to evaluate the induced dipoles.

The molecular dynamics simulations were performed on a system consisting of a chloride ion, 1429 water molecules, and 401 dichloromethane molecules in a rectangular simulation cell with linear dimensions of 35 × 35 × 70 Å. This system yields liquid densities of 0.997 and 1.32 g/cm$^3$ for water and dichloromethane at room temperature, respectively. The initial configuration of the ion transport across the liquid−liquid interface is obtained from previous neat water/dichloromethane, liquid−liquid simulations.[13] The ion is initially placed in the bulk water region and the interface is chosen to be perpendicular to the $z$-axis as shown in Figure 2. The water molecules are located in the region of $z > 35$ Å, while the dichloromethane molecules occupy the region of $z < 35$ Å. The simulations are performed at a constant volume and temperature with periodic boundary conditions are applied in all three directions. The

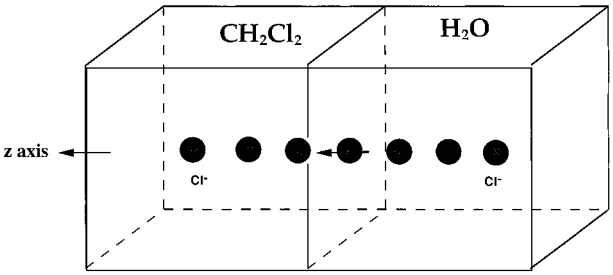


**Figure 2.** Schematic representation of the simulation cell for the transfer of a chloride ion across the $H_2O-CH_2Cl_2$ interface.

temperature of the system is maintained at 298 K by coupling the $H_2O$ and dichloromethane to separate external thermal baths with a time constant of 0.2 ps.[18] The initial velocity assigned to each atom is chosen from a Maxwell−Boltzmann distribution corresponding to the desired simulation temperature. During the molecular dynamics simulations, the SHAKE algorithm[19] is employed to fix the $H_2O$ and $CH_2Cl_2$ geometry by constraining all of the bond lengths. A time step of 2 fs is used in integrating the equations of motion.

The nonbonded interactions (i.e., Lennard-Jones, Coulombic, and polarization) are truncated at molecular center-of-mass separations. Specifically, the $H_2O-H_2O$, ion$-CH_2Cl_2$, and ion$-H_2O$, interactions are truncated at a molecular separation of 9 Å, while the $CH_2Cl_2-CH_2Cl_2$ and $CH_2Cl_2-H_2O$ interactions are truncated at longer distances of 11 and 10 Å, respectively, due to oscillations observed in the radial distribution functions at larger separations. Recently, Brooks and co-workers computed the equilibrium properties of the liquid−vapor interface of water and water−lipid interface using both spherical truncation and Ewald summation techniques. Although Brooks and co-workers observed some differences in the computed surface tensions and the electrostatic potential profiles, they have not studied the equilibrium properties of ionic solvation free energy at the interface.[20] Therefore, the extent to which the effect of using Ewald techniques on the free energy profile of ion transport across the liquid−liquid interface is unknown at this time. In this study, we are dealing with a single ion solvation free energy between two points that are well defined in space. Therefore, we expect the Ewald boundary conditions will play minor role in this calculation and their effects will not alter the physical meaning of the results of this study.

To evaluate the free energies associated with the transfer of an ion across the liquid−liquid interface, we used a constrained molecular dynamics technique similar to the approach used for ionic association.[21] The reaction coordinate for ion transfer can be considered as the $z_s$ position of the ion. The Helmholtz free energy difference, $\Delta F(z_s)$, between a state where the ion is located at $z_s$, $F(z_s)$, and a reference state where the ion is at $z_0$, $F_0$, is simply

$$\Delta F(z_s) = F(z_s) - F_0 = -\int_{z_0}^{z_s} \langle f_z(z_s') \rangle dz_s' \qquad (4)$$

where $f_z(z_s')$ is the $z$ component of the total force exerting on the ion at a given $z$ position, $z_s'$, averaged over the canonical ensemble. Here, $F_0$ is chosen as the free energy of the system with the ion located in the bulk water region. During the simulation, the $z$ coordinate of the ion was reset to the original value after each dynamical step, and the average force acting on the ion then was evaluated. The average forces are subsequently integrated to yield the free energy profile or the PMF. For the calculations reported in this paper, the position of the ion ranges from $z = 22$ to 50 Å, with a position increment of 1.0 Å. The total simulation time at each ion position was at least 200 ps with 100 ps for equilibration. We found the average forces for a given ion position converged within a 100 ps simulation time as demonstrated in Figure 3.

## III. Results and Discussion

In Figure 4, the average PMF for transferring a chloride ion across the $H_2O/CH_2Cl_2$ liquid−liquid interface at 298 K as a function of $Z$-axis normal to the interface is shown. In addition, both the forward and reverse simulations are also included in the figure. Upon examining the free energy profile, we found that it exhibits a monotonic increase from the aqueous phase into the organic phase. The computed free energy undergoes major changes as the ion begins to cross the interface. No barrier was found at the liquid−liquid interface. The change in free energy is positive and it can be understood by comparing the $Cl^--H_2O$ and $Cl^--CH_2Cl_2$ dimer potential energy surfaces shown in Figure 1. It is clear that the preferred phase for the chloride ion is the aqueous phase rather than the nonaqueous phase. The estimated free energy of transfer is $14 \pm 2$ kcal/mol, which is in qualitative agreement with the experimentally reported value of $10 \pm 1$.kcal/mol.[22] The difference can be attributed to the deficiencies in the $Cl^--H_2O$ and $Cl^--CH_2Cl_2$ potential energy surfaces. The agreement with the experimental data can be improved by reoptimizing the ion potential parameters to reproduce the experimental ion free energy of solvation in water and organic solvent.

As we reported previously, the PMFs were decomposed into energy contributions that correspond to the individual ion−solvent interactions. These energy contributions indicate that the computed free energy of ion transfer is the result of a competition between the Lennard-Jones and the electrostatic interactions (Coulombic and polarization). This finding is significantly different from the transferring of a neutral solute molecule (methane or chloroform) across this interface, where the free energy required creating a cavity is a major contribution.[23]

During the transfer process, we monitored the coordination number for the chloride ion as a function of the $Z$-axis normal to the interface. As the chloride ion moved across the interface, the first hydration shell of the ion began to be reduced as shown in Figure 5. The characteristic of this figure is clearly similar to the computed free energy profile. For instance, the free energy profile moves upward while the coordination number moves downward. Thus, an ion transfer mechanism that involves changes in the hydration shell of the ion has been demonstrated. This finding is in excellent agreement with recent experimental study by Osakai et al.[24] These authors measured the Gibbs free energy of ion transfer between water and nitrobenzene interface for various ions. By using the Karl Fisher method,[24] they also measured the water content in nitrobenzene and found a fraction of water associated with the ion in the nitrobenzene liquid phase. For example, the coordination number of a sodium ion is approximately 6 in water. The coordination number deceased to approximately 4 when the ion is transferred to nitrobenzene. In Figure 6, a snapshot was taken from the molecular dynamics simulation when the chloride ion was located in the $CH_2Cl_2$ liquid phase, 13 Å away from the interface. As can be seen from the features of Figure 6, our results very closely agree with the model suggested by Osakai et al.[24]

We examined the interface for various chloride-ion positions along the $Z$-axis and found some distortion to exist as the chloride ion moves from the aqueous phase to the nonaqueous phase. The most severe case of distortion occurs when the ion

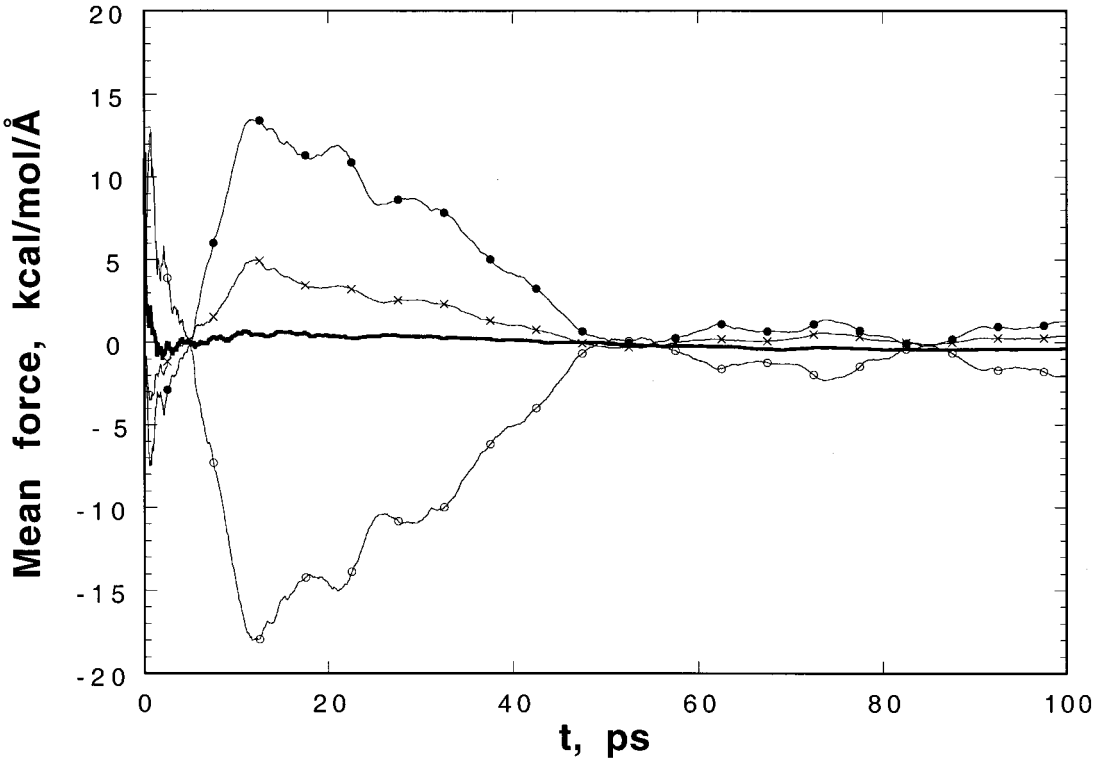


**Figure 3.** Cumulative forces (for a given ion position) acting on the ion as a function of time. Solid line (total), solid circles (polarization), open circles (Lennard-Jones), and open circle (Coulombic).

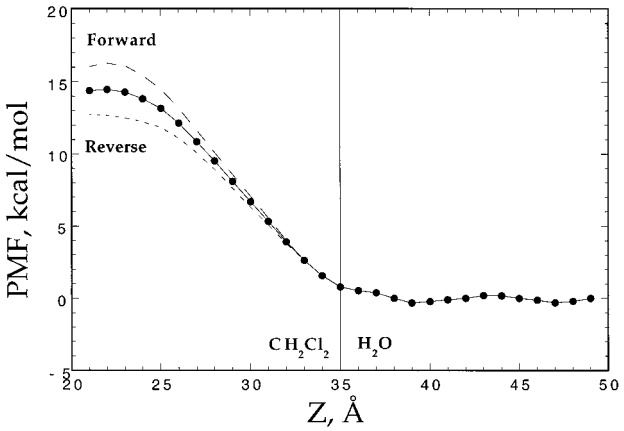


**Figure 4.** Computed free energy profile of transferring a chloride ion across a water−dichloromethane liquid−liquid interface.

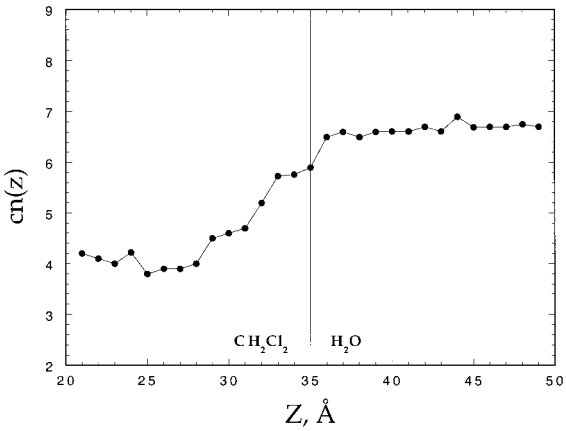


**Figure 5.** Computed hydration numbers of the chloride ionas a function of *z*-axis normal to the interface.

in located deep inside the nonaqueous phase. The computed density profiles for water and dicholomethane when the chloride is at the interface are shown in Figure 7. These results are very similar to the corresponding results obtained from the pure liquid−liquid interface. As already mentioned in previous work by Benjamin,[6] at short distances (<12 Å), fingering effects were observed as the chloride ion moves into the nonaqueous phase. Due to the strong hydrogen-bonding network between water molecules, these fingering effects persist for at least a few nanoseconds in our simulations. The fingering effects disappear as the chloride ion moves further into the $CH_2Cl_2$ liquid phase.

As noted in our previous study of liquid−liquid interface,[13] one advantage of using polarizable potential models is that it can more realistically account for the electrostatic properties of molecules in inhomogeneous environments. Thus, to understand the effect of polarization on the electrical properties of the $H_2O$ and $CH_2Cl_2$ molecules, we calculated the average dipole moments of the $H_2O$ and $CH_2Cl_2$ molecules as a function of the *z* axis and ion positions. The results are shown in Figure 8 when the ion is at the center of the liquid−liquid interface. The dipole moments were computed using 1-Å-thick liquid slabs. Figure 8 shows that the $H_2O$ molecules far from the interface (i.e., $Z = 40-70$ Å) have an average dipole moment of 2.8 D, which is very close to the value obtained for bulk $H_2O$. The dipole moments of the $H_2O$ molecules residing within the interface (∼30−40 Å) decrease monotonically as they approach the interface and are close to their gas-phase values. This result would be expected because of changes in the hydrogen bonding patterns and the electric field of water molecules near the interface. In addition, another factor that influences the reduction in the induced dipole is the smaller density of water (and thus a lower local electric field). The computed average dipole moment of $CH_2Cl_2$ molecules, as a function of the *Z*-coordinate, is also included in Figure 8. As expected, due to the strong field from water molecules near the interface, the average dipole moment of $CH_2Cl_2$ molecules are enhanced considerably.

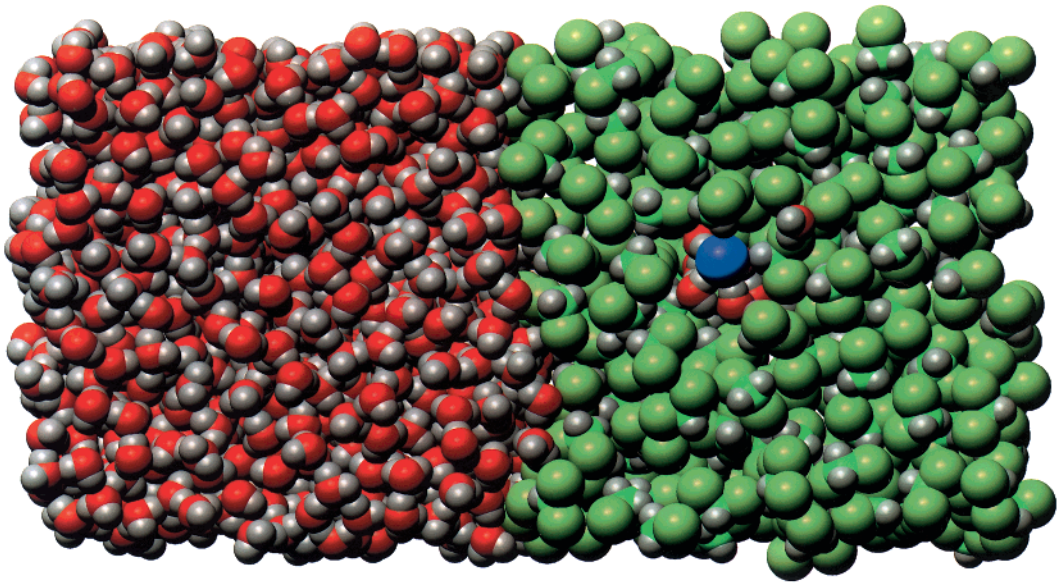

**Figure 6.** Snapshots taken at the end the molecular dynamics simulations when the chloride ion was moved away from the interface into the $CH_2Cl_2$ liquid phase.

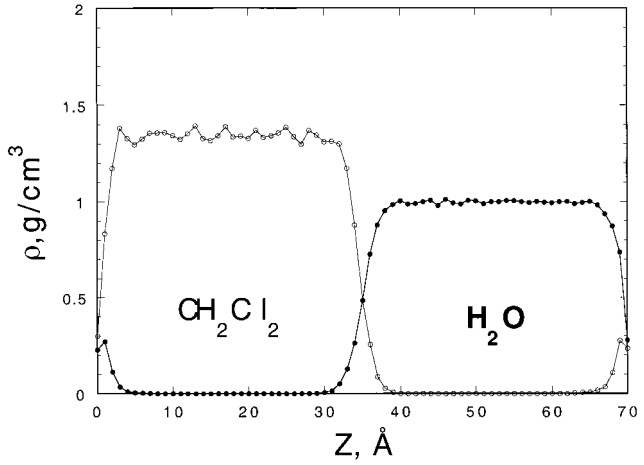


**Figure 7.** Computed density profiles of $CH_2Cl_2$ (open circles) and $H_2O$ (solid circles) at 298 K from molecular dynamics simulations, when the chloride ion is at the liquid−liquid interface.

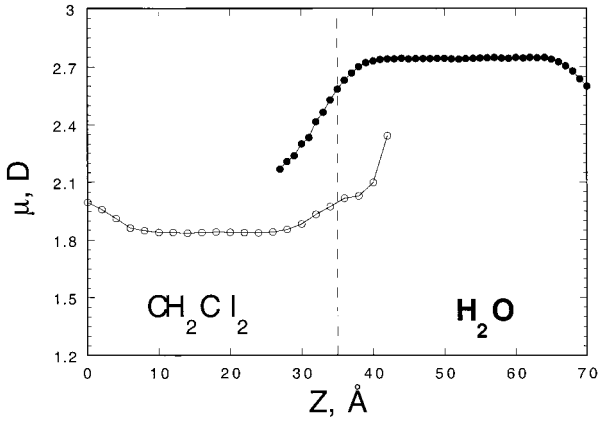


**Figure 8.** Average dipole moment of water and dichloromethane molecules as a function of the *Z*-axis, when the chloride ion is at the liquid−liquid interface.

## IV. Conclusions

In this work, we used molecular dynamics techniques and mean force approaches to compute the ion transfer free energy for a water−dichloromethane system. Based on our results, we have proposed a mechanism that describes the transport of a chloride ion across the liquid−liquid interface of this system. We used polarizable potential models to describe the interactions among the species, and we carried out the calculations in both the forward and reverse directions to evaluate the differences in the free energy profiles. The computed ion transfer free energy is 14 ± 2 kcal/mol, which is in qualitative agreement with the experimentally reported value of 10 ± 1 kcal/mol. The agreement can be improved significantly by refining the potential parameters for ion−water and ion−organic solvent interactions. A smooth transition from the aqueous phase to the nonaqueous phase on the free energy profile clearly indicates that the ion transfer mechanism is a nonactivated process. The computed hydration number for the chloride ion indicates that some water molecules are associated with the ion inside the nonaqueous phase. Our results are in excellent agreement with the results obtained from experiments and support the ion transfer mechanism proposed recently by Osakai et al.[24]

One important finding in this study is that no interfacial minimum is observed in the free energy profile for the water−dichloromethane system we studied. Thus, we can view the mechanism of ion transport across the interface of this system as a simple diffusive process. This result is far different from the conclusion drawn by Benjamin in his study of the mass transfer of chloride ion across the water−dichloroethane interface. This happens because the nature of the solvent structure was not taken into account fully in Benjamin's PMF calculations. In this calculation, the electrostatic free energies were calculated under nonequilibrium conditions. Atomistically, the solvation shells of the chloride ion did not have enough time to equilibrate as it crosses the liquid−liquid interface (i.e., the equilibrium configurations and energies have never been achieved). Therefore, the free energy differences were not sampled adequately. However, Schweighfer and Benjamin recently reported on their study of the transport of ammonium ions across the water−nitrobenzene liquid−liquid interface.[7] In their work, they found no barrier when the system is fully equilibrated.

For this study, we did not consider counterion effects on ion transport across the interface. In the past, we examined the role of the counterion on the ion−crown ether association in water. Those simulation studies indicated that including the counterion

lowers the free energy profile, but the characteristics of the profile remains the same. In future work on the liquid−liquid interface, we will include the counterions and Ewald summation techniques to evaluate their effects on the PMFs and the fingering phenomenon.

Explicitly incorporating polarization effects into potential model is still an evolving science. We believe that the simulations of ion solvation at the interface with explicitly including polarization effects are important because at the interface, the water dipole moments are significantly different from bulk values (i.e., $\mu \sim 2.0$ D at the interface and $\mu \sim 2.7$ D in the bulk liquid). Therefore, the interactions between solute−solvent at the interface will have effects on the computed results (i.e., free energy of solvation or spectroscopic properties of solute solvation at the interface).

**Acknowledgment.** This work was performed in the Environmental Molecular Sciences Laboratory (EMSL) at Pacific Northwest National Laboratory under the auspices of the Division of Chemical Sciences, Office of Basic Energy Sciences, U.S. Department of Energy. Pacific Northwest National Laboratory is operated by Battelle for the Department of Energy. Computer resources were provided by the Division of Chemical Sciences and by the Scientific Computing Staff, Office of Energy Research, at the National Energy Research Supercomputer Center (Berkeley, California). Operation of EMSL is supported by the DOE's Office of Biological and Environmental Research.

## References and Notes

(1) Berkowitz, M.; Karim, O. A.; McCammon J. A.; Rossky P. J. *Chem. Phys. Lett*. **1984**, *105*, 577. Smith, D. E.; Dang, L. X. *J. Chem. Phys.* **1994**, *101*, 7873.

(2) Dang, L. X. *J. Am. Chem. Soc.* **1995**, *117*, 6954.

(3) Young W. S.; Brooks, C. L. *J. Chem. Phys.* **1994**, *106*, 7873.

(4) Jorgensen, W. L.; Severance D. L. *J. Am. Chem. Soc.* **1990**, *112*, 4768.

(5) Haag, W. R.; Yao, C. C. D. *Environ. Sci. Technol.* **1992**, *26*, 1005. U.S. Department of Energy, Office of Environmental Management, FY 1995 Technology Development Needs Summary, **1994**, p 2−17.

(6) Benjamin, I. *Science* **1993**, *261*, 1558.

(7) Schweighfer, K.; Benjamin, I. *J. Phys. Chem. A* **1999**, *103*, 10274.

(8) Lauterbach, M.; Engler, E.; Muzet, N.; Troxler, L.; Wipff, G. *J. Phys. Chem. B* **1998**, *102*, 245.

(9) Fernandes, P. A.; Natalia, M. Cordeiro, D. S.; Gomes, J. A. N. F. *J. Phys. Chem. B* **1999**, *102*, 245; Fernandes, P. A.; Natalia, M. Cordeiro, D. S.; Gomes, J. A. N. F. *J. Phys. Chem. B* **2000**, *104*, 2390.

(10) Dang, L. X. *J. Phys. Chem. B* **1999**, *103*, 8195.

(11) Dang, L. X.; Chang, T.-M. *J. Chem. Phys.* **1997**, *106*, 8149.

(12) Murphy, W. *J. Chem. Phys.* **1977**, *67*, 5877.

(13) Dang, L. X. *J. Chem. Phys.* **1999**, *110*, 10113.

(14) Applequist, J.; Carl, J. R.; Fung, K.-K. *J. Am. Chem. Soc.* **1972**, *94*, 2952.

(15) Hansen, J. P.; McDonald, I. R. *Theory of Simple Liquids*; Academic Press: London, 1986.

(16) Chang, T.-M.; Dang, L. X. *J. Chem. Phys.* **1996**, *104*, 6772.

(17) Xantheas, S. *J. Phys. Chem.* **1995**, *100*, 9703.

(18) Rich, S. W.; Stuart, S. J.; Berne, B. J. *J. Chem. Phys.* **1994**, *101*, 6141. Stuart, S. J.; Berne, B. J. *J. Phys. Chem.* **1999**, *103*, 10300. Stuart, S. J.; Berne, B. J. *J. Phys. Chem.* **1996**, *100*, 11934. Stuart, S. J.; Berne, B. J. *J. Am. Chem. Soc.* **1996**, *118*, 672.

(19) Berendsen, H. J. C.; Postma, J. P.; Di Nola, A.; Van Gunsteren, W. F.; Haak, J. R. *J. Chem. Phys.* **1984**, *81*, 3684. Rykaert, J. R.; Ciccotti, G.; Berendsen, H. J. C. *J. Comput. Phys.* **1977**, *23*, 327.

(20) Feller, S. E.; Pastor, W. R. Rojnuckarin, A.; Boguszerara, S.; Brooks, B. *J. Phys. Chem.* **1996**, *100*, 17011.

(21) Smith, D. E.; Dang, L. X. *J. Chem. Phys.* **1994**, *100*, 3757.

(22) Marcus, Y. *Pure Appl. Chem.* **1983**, *55*, 977.

(23) Chang, T.-M.; Dang, L. X. *J. Chem. Phys.* **1998**, *108*, 2.

(24) Osakai, T.; Ogata, A.; Ebina, K. *J. Phys. Chem. B* **1997**, *101*, 8341.